PHYSICAL REVIEW B VOLUME 41, NUMBER 1 1 JANUARY 1990

Magnetoresistance and the spin-flop transition in single-crystal La_2CuO_{4+y}

Tineke Thio,* C. Y. Chen,* B. S. Freer,*† D. R. Gabbe, H. P. Jenssen, M. A. Kastner,*
P. J. Picone, and N. W. Preyer*
Center for Materials Science and Engineering, Massachusetts Institute of Technology, Cambridge, Massachusetts 02139

R. J. Birgeneau*
Brookhaven National Laboratory, Upton, New York 11973
(Received 29 June 1989)

Measurements are reported of the magnetoresistance (MR) for fields up to 23 T in La_2CuO_4 single crystals, which order antiferromagnetically at $T_N \sim 240$ K, and in which the conductivity at low temperature is characterized by hopping in localized states. Using the MR, the phase diagram of the spin-flop transition, observed when the magnetic field is applied parallel to the zero-field staggered magnetization, is mapped out. Two transitions of the background Cu^{2+} spins are observed, which are governed by the symmetric and antisymmetric anisotropic components of the superexchange tensor. The antiferromagnetic propagation vector changes from $\boldsymbol{\tau} \| \mathbf{a}$ at zero field to $\boldsymbol{\tau} \| \mathbf{c}$ at the highest fields. This subtle change in the ordering of the Cu^{2+} spins is accompanied by a large enhancement of the interlayer hopping conductivity up to a factor 2. We show that the magnetoconductance is proportional to the three-dimensional staggered moment with $\boldsymbol{\tau} \| \mathbf{c}$ direction. In an appendix we discuss the possible relevance of these results to the behavior of superconducting $La_{2-x}(Sr,Ba)_xCuO_4$.

I. INTRODUCTION

High-temperature superconductivity occurs in lamellar cuprates when doping introduces a sufficiently high density of excess holes or electrons into the CuO_2 layers. In many theoretical models, the pairing necessary for superconductivity involves the coupling of the charge carriers to the Cu^{2+} spins. In light of this, the study of the lightly doped, insulating antiferromagnetic state is important, because, in the latter, the density of charge carriers can be sufficiently low that the interaction between them is small relative to their interaction with the Cu^{2+} spins.

Materials in the $La_{2-x}(Sr,Ba)_xCuO_4$ system, in which high-T_c superconductivity was first discovered[1] have the simplest structure, so they are ideal for studying the physics of the CuO_2 layers. Undoped La_2CuO_4 is a model two-dimensional (2D) $S=\frac{1}{2}$ Heisenberg antiferromagnet.[2,3] Because of weak interlayer coupling, the spins order three dimensionally at temperatures close to room temperature. The in-plane nearest-neighbor interaction between the Cu^{2+} spins in La_2CuO_4 is described by the Heisenberg Hamiltonian to an unusually high degree of accuracy: The anisotropies are several orders of magnitude smaller than the nearest-neighbor exchange.[4,5]

Previous experiments[6,7] have demonstrated that the hopping conductivity in single crystals of La_2CuO_{4+y} is sensitive to the interlayer magnetic order of the Cu^{2+} spins; consequently, the magnetoresistance can be used as a probe of the magnetic order. This is particularly valuable because, as shown in this work, the spin-flop transitions occur at fields at which magnetization measurements are difficult.

In this paper we report magnetoresistance (MR) measurements on pure single crystals of La_2CuO_{4+y} for magnetic fields up to 23 T applied *parallel* to the CuO_2 planes. When an external field is applied in the direction of the staggered magnetization ($\mathbf{M}^{\dagger} \| \mathbf{c}$ in orthorhombic notation, space group *Cmca*), a feature in the MR indicates a spin-flop transition, dominated by the Dzyaloshinsky-Moriya antisymmetric exchange. Because of the peculiar nature of the antisymmetric exchange, a second feature is observed at a higher critical field, which provides a measure of the out-of-plane anisotropy. From an extrapolation of the observed critical fields to $T=0$ we find values for the anisotropies which confirm earlier measurements[4-6] of the spin Hamiltonian.

The MR provides new insight into the coupling between the excess holes and the background magnetism. We find that the observed MR arises from the interlayer hopping conductivity which is proportional to the total staggered moment with propagation vector $\boldsymbol{\tau}$ in the $\mathbf{c}$ direction, both for the spin-flop transition and for the weak ferromagnetic (WF) transition observed for $\mathbf{H} \| \mathbf{b}$. In both transitions, $\boldsymbol{\tau}$ changes from $\boldsymbol{\tau} \| \mathbf{a}$ at $H=0$ to $\boldsymbol{\tau} \| \mathbf{c}$ at the highest fields. The distinction between the two in-plane axes $\mathbf{a}$ and $\mathbf{c}$ is very small, since the deviation from the tetragonal structure is only $\sim 0.5\%$.[8] The change in the Cu^{2+} spin ordering is therefore quite subtle; surprisingly, it is accompanied by a large enhancement of the hopping conductivity, up to a factor 2.

The format of this paper is as follows: In Sec. II we describe the samples and the details of the experimental method; the results are presented in Sec. III. In Sec. IV we discuss in detail the spin-flop transition in La_2CuO_4 and we demonstrate that the ordering of the Cu^{2+} spins influences the hopping conductivity. We summarize our findings in Sec. V. In the Appendix we discuss the possible relevance of these results to the more heavily doped superconducting regimes of $La_{2-x}Sr_xCuO_4$ and especially $La_{2-x}Ba_xCuO_4$.

II. EXPERIMENTAL DETAILS

The samples used for this experiment are the same as those used in the WF transition experiments.[6] They are large single crystals of pure La_2CuO_{4+y} grown by the top-seeded solution growth method using CuO flux.[9] The crystals have transport properties characteristic of doped semiconductors on the insulating side of the insulator-to-metal transition.[10,11] We estimate[10] that the samples contain a density of $\sim 4\times 10^{19}$ cm^{-3} holes because of unintentional doping by acceptors, probably[12] O_2^-, which is sufficient to reduce the Néel temperature from the value at stoichiometry ($T_N = 320$ K), to $T_N = 240$ K. We determine the Néel temperature from the magnetic susceptibility $\chi(T)$, which has a sharp peak at T_N originating from the antisymmetric exchange.[6] This peak is expected for **H**||**b** or **H**||**c**, but not for **H**||**a**.

It should be kept in mind that the crystals are grown at high temperature in the tetragonal phase. When they are cooled through the tetragonal-orthorhombic phase transition in the absence of stress, they have twin domains. For this reason we label a magnetic field applied in an orthorhombic in-plane direction **H**||**a**,**c**. It is possible to obtain a single-domain sample by cooling a crystal through the tetragonal-to-orthorhombic transition in the presence of a uniaxial stress. In such a sample, $\chi(T)$ indeed has no peak at the Néel temperature for **H**||**a**. In an as-grown sample, we have measured the uniform magnetic moment as a function of field **H**||**a**,c for fields up to 20 T, using a vibrating susceptometer.

To measure the magnetoresistance, the sample is mounted on a variable-temperature cold finger and placed in the center of a Bitter magnet. Using a conventional four-probe geometry with the current perpendicular to the CuO_2 planes, the resistance is measured as a function of magnetic field for fields up to 23 T at typical sweep rates of 0.08 T/s.

Some of the samples used in this experiment appear to have small cracks, which are visible by eye or under an optical microscope, and which make it difficult to measure the absolute conductivity. In high-quality samples, which have no observable cracks, the conductivity is highly anisotropic.[10] We use the Montgomery method[13] to measure the anisotropy and to determine the change in the conductivity tensor at the WF transition. Ideally, the Montgomery method requires line contacts at four edges of a brick-shaped sample. The finite size of our contacts ($\sim 10\%$ of the dimension of our samples) introduces a small uncertainty in the conductivity measurements.

III. RESULTS

Figure 1(a) shows the MR normalized to the zero-field resistance R_0 for **H**||**a**,**c**. At all temperatures the resistance decreases monotonically with increasing field; the overall change in resistance can be as large as a factor of ~ 2 at $T=24$ K. At low T the MR has knees at two distinct critical fields; at the highest temperatures only one transition is observed. These features appear more clearly in the derivative dR/dH, plotted as a function of magnetic field in Fig. 1(b); the features are free of hysteresis.

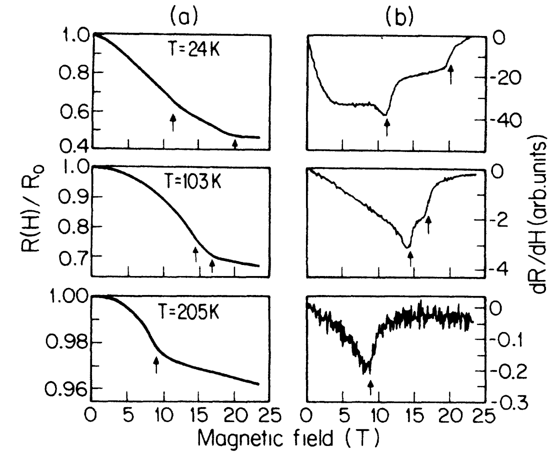

FIG. 1. (a) Magnetoresistance normalized to zero-field resistance R_0 for **H**||**a**,**c**; (b) derivative of the MR as a function of field. Arrows indicate critical fields.

The critical fields are plotted versus temperature to generate the phase diagram shown in Fig. 2. At low temperature, two distinct phase boundaries are seen for **H**||**a**,**c**. The zero-temperature extrapolations of the critical fields are $H_1(0)=10.5\pm1.0$ T and $H_2(0)=20.5\pm1.0$ T. The two boundaries merge at a multicritical point at $T_{mc}\sim 120$ K. Above T_{mc} there is only one phase boundary which tends to zero field at $T_N=240$ K, the Néel temperature of the sample. In crystals which order antiferromagnetically at 200 K$<T_N<$260 K, $H_1(0)$ and $H_2(0)$ are not appreciably different. Figure 2 includes the phase boundary observed when the magnetic field is

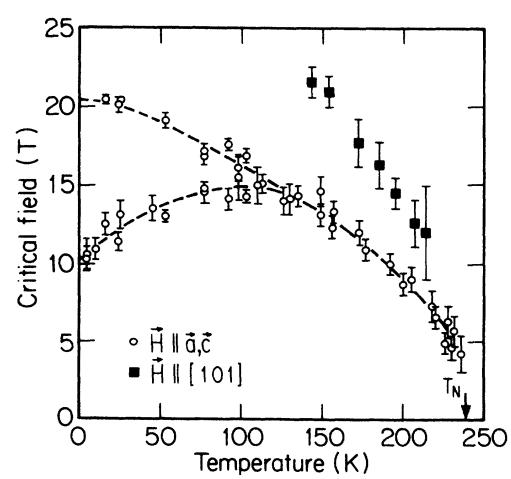

FIG. 2. Temperature dependence of the critical fields from the MR for **H**||**a**,**c** (circles) and **H**||[1 0 1] (solid squares). The dashed lines are guides to the eye.

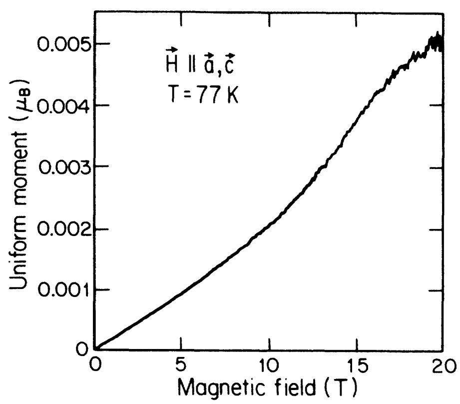

FIG. 3. Uniform ferromagnetic moment $M_+^F(H)$ as a function of field H∥a,c; $T=77$ K.

applied in the [1 0 1] in-plane direction. At the highest temperatures we observe one phase boundary, which lies at fields ~ 1.5 times higher than those observed for **H**∥**a**,**c**. At low T no transitions are observed within the 23 T range of our experiment.

The field dependence of the uniform ferromagnetic moment at $T=77$ K, with **H**∥**a**,**c**, is plotted in Fig. 3. The moment increases superlinearly with field above $H \sim 5$ T, and has a knee at $H \sim 17$ T, close to the value of H_2 at this temperature.

As can be seen in Fig. 1, the MR saturates above ~ 21 T. The magnitude

$$[R(23\ \mathrm{T})-R_0]/R_0=\Delta R/R_0$$

varies from run to run, presumably because of cracks in some crystals, although the temperature dependence is the same. There is, however, an upper limit to the measured $\Delta R/R_0$, and the largest $\Delta R/R_0$ observed was reproduced in several runs. Using data from these runs we plot $\Delta\sigma/\sigma_0$, the overall change in the conductivity, in Fig. 4. $\Delta\sigma/\sigma_0$ is as large as ~ 1.25 at $T=24$ K, and goes to zero at T_N. The overall change in resistance for **H**∥**a**,**c** is the same as that found in the MR of the same sample, for the WF transition,[6] observed for **H**∥**b**; data from the latter are included in the figure for comparison. This similarity strongly suggests that the MR in both transitions arises from the same coupling mechanism of the holes to the Cu^{2+} spins.

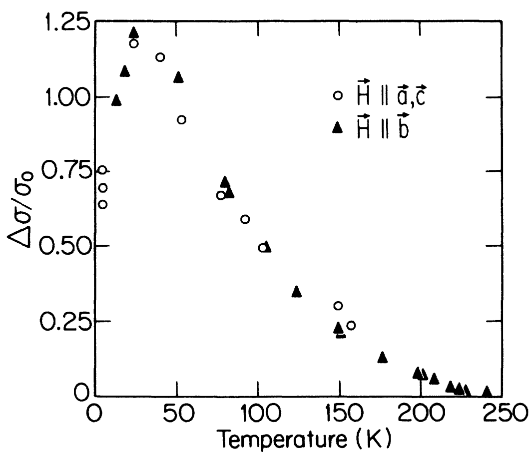

FIG. 4. Temperature dependence of the overall change of the conductivity for H∥a,c (circles) and H∥/b (solid triangles).

In Fig. 5 are plotted the temperature dependence of the anisotropy of the conductivity at zero field and of the MR for **H**∥**b**, measured with the Montgomery method[13] on a crystal which has no observable cracks. Both σ_a/σ_b, the anisotropy of the conductivity at $H=0$ [Fig. 5(a)], and $(\Delta\sigma_b/\sigma_b)/(\Delta\sigma_a/\sigma_a)$, the anisotropy of the *relative* MR [Fig. 5(b)], appear to be weakly temperature dependent at low T and increase rapidly with T for $T > 50$ K, whereas $\Delta\sigma_b/\Delta\sigma_a$, the anisotropy in the *absolute* MR, is only weakly dependent on T over the entire temperature range [Fig. 5(c)].

IV. DISCUSSION

A. Spin-flop transition

We briefly review the relevant magnetic parameters in La_2CuO_4. In orthorhombic notation, the in-plane nearest-neighbor exchange is written $H_{ij}=\mathbf{S}_i\cdot\overleftrightarrow{\mathbf{J}}\cdot\mathbf{S}_j$, where

$$\overleftrightarrow{\mathrm{J}}=\begin{bmatrix} J^{aa} & 0 & 0 \\ 0 & J^{bb} & J^{bc} \\ 0 & -J^{bc} & J^{cc} \end{bmatrix} . \qquad (1)$$

Here $J_{\mathrm{nn}}=\frac{1}{3}(J+J^{bb}+J^{cc})\approx 128$ meV.[14] Because $J^{cc}=J^{aa}>J^{bb}$, there is an out-of-plane gap in the magnon

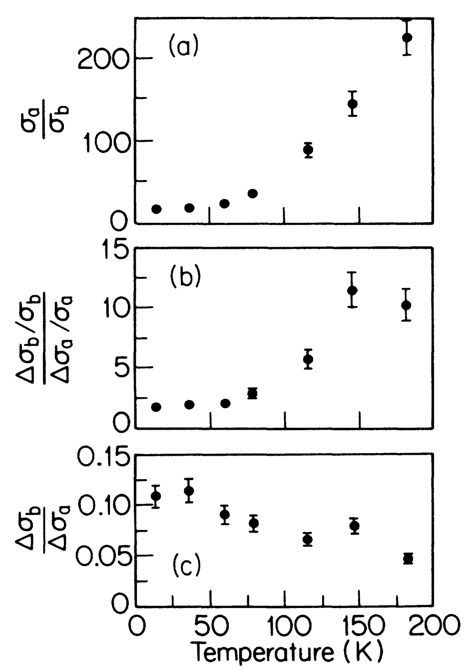

FIG. 5. Temperature dependence of the anisotropy of (a) the conductivity at zero field; (b) the relative overall magnetoconductance; (c) the absolute overall magnetoconductance. H∥b.

spectrum

$$E_A^b = zS[2J_{\mathrm{NN}}(J^{cc}-J^{bb})]^{1/2} ,$$

where $z=4$ is the number of nearest neighbors. The antisymmetric elements J^{bc} arise from a Dzyaloshinsky-Moriya[15,16] interaction that is allowed in the orthorhombically distorted crystal structure.[6,17] J^{bc} introduces an in-plane anisotropy gap $E_A^a = zJ^{bc}S$; infrared absorption and neutron scattering measurements indicate $E_A^a = 1.1 \pm 0.3$ meV and $E_A^b = 2.5 \pm 0.5$ meV.[4,5] These anisotropies cause the staggered moment at zero field to lie in the orthorhombic **c** direction [see Fig. 6(b)]. The spins cant in the **b** direction, giving rise to weak ferromagnetism which is hidden because the effective interlayer exchange $J_\perp$ is antiferromagnetic (AF). The interlayer order determines the direction of the AF propagation vector τ: For AF interlayer order, $\tau \| \mathbf{a}$, and for ferromagnetic interlayer order, $\tau \| \mathbf{c}$.[7]

In a conventional (two-sublattice) anisotropic antiferromagnet, only one spin-flop transition is seen, and it is dominated by the smallest anisotropy. However, in La_2CuO_4 the MR shows evidence of effects of both the out-of-plane anisotropy $J^{cc}-J^{bb}$ and the antisymmetric exchange J^{bc}. To understand why *both* gaps are visible, consider the $T=0$ behavior of the Cu spins in the presence of an external field. We include the effects of the interlayer exchange as well as the nearest-neighbor exchange of Eq. (1). Since both couplings are antiferromagnetic, the magnetic unit cell contains four spins in two inequivalent CuO_2 layers. In the presence of a magnetic field the effective Hamiltonian for the four-sublattice unit cell of Fig. 6 is

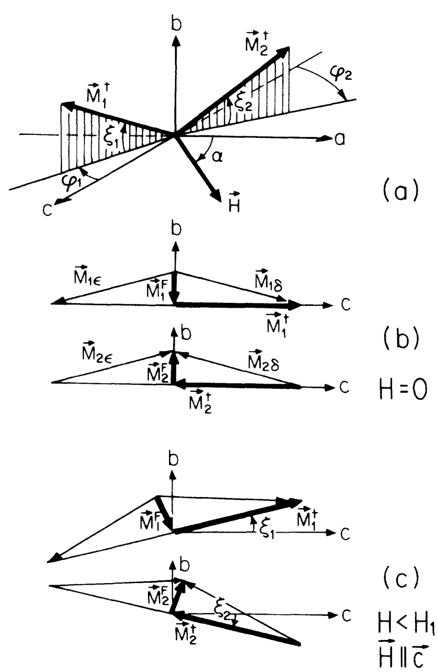

FIG. 6. (a) Directions of staggered moment $\mathbf{M}_i^\dagger$ and applied field $\mathbf{H}$; magnetic moments in the four-sublattice unit cell, projected along the **a** direction, for (b) $H=0$ and (c) $\mathbf{H}\|\mathbf{c}$, $0<H<H_1$.

$$\begin{aligned} H_{\text{unit cell}} &= z\mathbf{S}_{1\delta}\cdot\overleftrightarrow{\mathbf{J}}\cdot\mathbf{S}_{1\epsilon} - g\mu_B\mathbf{H}\cdot(\mathbf{S}_{1\delta}+\mathbf{S}_{1\epsilon}) \\ &\quad + z\mathbf{S}_{2\delta}\cdot\overleftrightarrow{\mathbf{J}}\cdot\mathbf{S}_{2\epsilon} - g\mu_B\mathbf{H}\cdot(\mathbf{S}_{2\delta}+\mathbf{S}_{2\epsilon}) \\ &\quad + z'J_\perp(\mathbf{S}_{1\delta}\cdot\mathbf{S}_{2\delta}+\mathbf{S}_{1\epsilon}\cdot\mathbf{S}_{2\epsilon}) , \end{aligned} \tag{2}$$

where 1 and 2 denote the first and second layers, respectively, and δ and ϵ denote, respectively, the corner and face-centered spins within a single CuO_2 plane. $J_\perp$ is the effective interlayer exchange ($J_\perp > 0$) and $z'=2$ is the effective number of interlayer nearest neighbors. We consider the general case, in which we allow the field to point in an arbitrary direction within the CuO_2 plane defined by the angle α between the field and the **a** axis [see Fig. 6(a)].

For two nearest-neighbor spins in the ith layer, one can define a staggered moment $\mathbf{M}_i^\dagger = (\mathbf{M}_{i\delta}-\mathbf{M}_{i\epsilon})/2$ and a ferromagnetic moment $\mathbf{M}_i^F = (\mathbf{M}_{i\delta}+\mathbf{M}_{i\epsilon})/2$. The direction of the staggered moment is defined by the out-of-plane angle ξ_i and in-plane ϕ_i defined in Fig. 6(a): At $H=0$, $\phi_i = \xi_i = 0$. To find the field dependence of the angles ϕ_i and ξ_i at $T=0$, the Hamiltonian of Eq. (2) is minimized, using a mean-field approximation, with respect to $\mathbf{M}_i^F$ and $\mathbf{M}_i^\dagger$. Noting that $\mathbf{M}_i^\dagger \perp \mathbf{M}_i^F$ and $\mathbf{M}_i^F \ll \mathbf{M}_i^\dagger$, we find the following field dependence of the angles ξ_i and ϕ_i in the two layers $i=1,2$:

$$\begin{aligned} &\xi_1 = \xi_2 = \xi, \quad \phi_1 = \phi_2 = \phi , \\ &\tan 2\phi = \frac{\sin 2\alpha}{\left[\dfrac{H_M}{H}\right]^2 + \cos 2\alpha} , \\ &\sin\xi = \frac{H_M H \sin\alpha}{2H_E H_A^b + 4H_E H_\perp - H^2\sin^2(\alpha-\phi) - H_M^2 \sin\phi} , \end{aligned} \tag{3}$$

where $g\mu_B H_E = zJ_{\mathrm{nn}}S$, $g\mu_B H_A^b = z(J^{cc}-J^{bb})S$, $g\mu_B H_M = zJ^{bc}S$, and $g\mu_B H_\perp = z'J_\perp S$. The field dependences of the angles ϕ and ξ are shown in Fig. 7 for the cases $\mathbf{H}\|\mathbf{c}$ ($\alpha=\pi/2$; solid line) and $\mathbf{H}\|[1\ 0\ 1]$ ($\alpha=\pi/4$; dashed line).

To gain some physical insight into this unusual spin-flop transition, we discuss heuristically the case $\mathbf{H}\|\mathbf{c}$ ($\alpha=\pi/2$). The solid line in Fig. 8 illustrates the trajectory of $\mathbf{M}_1^\dagger$ as a function of field. At zero field $\mathbf{M}_i^\dagger \| \mathbf{c}$ and $\mathbf{M}_1^\dagger = -\mathbf{M}_2^\dagger$ ($\tau\|\mathbf{a}$). The antisymmetric exchange creates a small ferromagnetic moment, $\mathbf{M}_i^F \| \mathbf{b}$, which is of opposite sign in adjacent layers [see Fig. 6(b)]. In the presence of a small external field, $\mathbf{M}_i^F$ will tend to align with the field, so the effect of the field $\mathbf{H}\|\mathbf{c}$ will be to rotate the staggered magnetization $\mathbf{M}_i^\dagger$ out of the plane [see Fig. 6(c)]. Since $\mathbf{M}_i^F$ points in opposite directions in neighboring layers, $\mathbf{M}_i^\dagger$ in adjacent layers will be rotated in opposite directions, so that energy is lost from the antiferromagnetic interlayer coupling $J_\perp$ as well as from the out-of-plane anisotropy $J^{cc}-J^{bb}$.

At low field, $\mathbf{M}_i^\dagger$ remains in the ($\mathbf{b},\mathbf{c}$) plane ($\phi=0$) to minimize the antisymmetric exchange energy. But when the magnetic field is large enough to overcome the antisymmetric exchange ($H=H_1$), $\mathbf{M}_i^\dagger$ flops into the ($\mathbf{a},\mathbf{b}$) plane: $\phi=\pi/2$, as shown in Fig. 7(a). Now $\mathbf{M}_i^\dagger \perp \mathbf{H}$ and the system lowers its energy from the external field at the

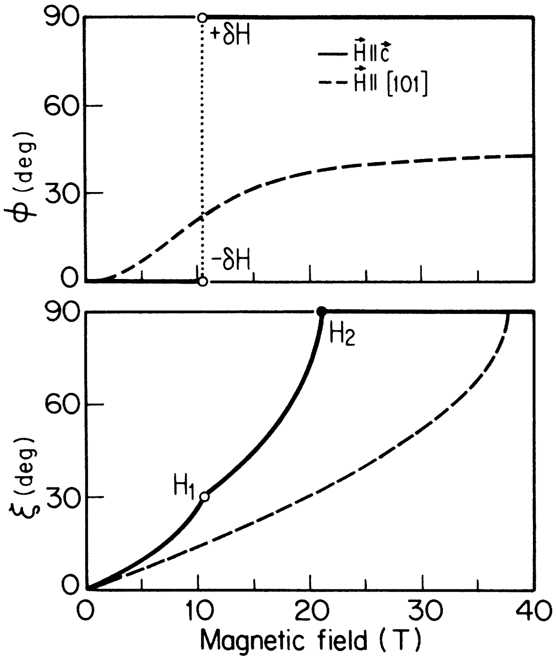

FIG. 7. Calculated field dependence of (a) the in-plane angle ϕ and (b) the out-of-plane angle ξ of the staggered moment, defined in Fig. 6(a), for $\alpha=\pi/2$ (solid line), and $\alpha=\pi/4$ (dashed line).

expense of the antisymmetric exchange. In this respect the first transition is like a conventional spin flop. However, in contrast to the conventional case, $\mathbf{M}_i^\dagger$ does not remain parallel to $\mathbf{H}$, even at the lowest fields. At the spin-flop transition, the out-of-plane angle ξ is nonzero; it is unchanged during the flop. However, for $H>H_1$, ξ continues to increase until it reaches its maximum value $\pi/2$ at a field H_2; for fields greater than H_2, $\mathbf{M}_i^\dagger$ remains parallel to $\mathbf{b}$. At very high fields this is the lowest-energy configuration because with $\mathbf{M}_i^\dagger \| \mathbf{b}$ and $\mathbf{M}_i^F \| \mathbf{c}$, the antisymmetric exchange and the field, $\mathbf{H}\|\mathbf{c}$, reinforce one another. Because J^{bc} has the same sign in adjacent layers, this configuration requires the interlayer magnetic order to be *ferromagnetic:* $\mathbf{M}_1^\dagger=\mathbf{M}_2^\dagger$, or $\tau\|\mathbf{c}$.

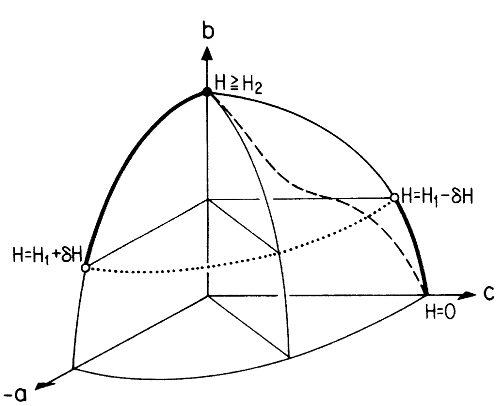

FIG. 8. Trajectory of $\mathbf{M}_1^\dagger$ for $\mathbf{H}\|\mathbf{c}$ ($\alpha=\pi/2$, solid line) and for $\mathbf{H}\|[1\ 0\ 1]$ ($\alpha=\pi/4$, dashed line).

As in the conventional spin flop, the transition at H_1 is discontinuous only if the angle between $\mathbf{H}$ and $\mathbf{M}_i^\dagger$ is very small.[18] When the field is applied off axis, both ϕ and ξ increase continuously, as shown by the dashed line in Figs. 7 and 8 for $\alpha=45°$. However, there is still a feature at the field for which $\mathbf{M}_i^\dagger$ becomes parallel to the $\mathbf{b}$ axis, in contrast to the conventional spin flop, in which no transition is observed at all when $\alpha=45°$. This explains why even with the field 45° off axis, we observe a phase boundary (see Fig. 2). That boundary lies at higher field than that for $\mathbf{H}\|\mathbf{a},\mathbf{c}$, consistent with the $\xi(H)$ calculated for the two directions as shown in Fig. 7(b).

For $\mathbf{H}\|\mathbf{c}$ the critical fields are

$$H_1=H_M\ ,$$
$$H_2=\frac{1}{H_M}(2H_EH_A^b+4H_EH_\perp-H_M^2)\ . \tag{4}$$

From the zero-temperature extrapolation of the lower phase boundary in Fig. 2, $H_1(0)=10.5\pm1.0$ T, we find a spin-wave gap $E_A^a=1.3\pm0.2$ meV. This value is to be compared to that measured in neutron scattering[4] ($E_A^a=1.0\pm0.3$) and infrared spectroscopy[5] ($E_A^a=1.1\pm0.3$ meV). Using the classical expression $H_M=zJ^{bc}S$ gives the value $J^{bc}=0.7\pm0.1$ meV. This value agrees to within experimental error with that measured in the WF transition[6] ($J^{bc}=0.8\pm0.3$ meV). To extract the out-of-plane anisotropy, we use $J_{\rm NN}=128$ meV, from two-magnon Raman scattering,[14] and $J_\perp=2$ μeV from the WF transition;[6] with $H_2(0)=20.5\pm1.0$ T, we find the out-of-plane gap

$$E_A^b=g\mu_B(2H_EH_A^b)^{1/2}=1.8\pm0.6\ \text{meV}\ ,$$

in agreement with the neutron scattering result ($E_A^b=2.5\pm0.5$ meV). From this we extract the out-of-plane anisotropy $J^{cc}-J^{bb}=3\pm2$ μeV.

It is, in general, very difficult to predict *a priori* the magnitude,[19] let alone the anisotropies of exchange constants. However, as shown in previous work,[6] in La_2CuO_4 the largest correction to the Heisenberg superexchange is the antisymmetric exchange which arises from first-order corrections due to spin-orbit coupling to excited state orbitals,[16] allowed by the orthorhombic crystal structure. The antisymmetric exchange is $J^{bc}\approx(\Delta g/g)\phi_0 J_{\rm NN}$, where the g shift is a measure of the strength of the spin-orbit coupling, and ϕ_0 is the tilt angle of the CuO_6 octahedra in the orthorhombically distorted phase. Corrections to the superexchange which are second order in the spin-orbit coupling typically give rise to symmetric anisotropies of order $\Delta J\approx(\Delta g/g)^2 J_{\rm NN}\approx 1$ meV, more than two orders of magnitude larger than the observed anisotropy $J^{cc}-J^{bb}$. Thus, corrections of the superexchange due to spin-orbit coupling are sufficient to explain the antisymmetric exchange, but they grossly overestimate the planar anisotropy. We have confirmed the conclusion from previous measurements[4] that the exchange anisotropies are much smaller than the exchange itself. Since the interlayer coupling $J_\perp$ is also very small, La_2CuO_4 is a model 2D $S=\frac{1}{2}$ Heisenberg antiferromagnet.

Our calculation of the spin-flop transition predicts the moments $\mathbf{M}_i^F$ in the two different layers $i=1,2$, as a function of field in the **a**,**c** plane. The uniform moment $\mathbf{M}_+^F=(\mathbf{M}_1^F+\mathbf{M}_2^F)/2$ is parallel to the applied field, and its magnitude is

$$M_+^F=\frac{(g\mu_B)^2}{2zJ_{\rm NN}}\{H[1-\cos^2\xi\sin^2(\alpha-\phi)]+H_M\sin\xi\sin\alpha\}\ , \tag{5}$$

where ϕ and ξ depend on H according to Eqs. (3).

With $\mathbf{H}\|\mathbf{a}$ ($\alpha=0$), the uniform moment $M_+^F(H)$ is linear in field, with slope $\chi_0=(2zJ_{\rm NN})^{-1}$, the perpendicular susceptibility. The calculated total moment for $\mathbf{H}\|\mathbf{c}$ is plotted with the solid line in Fig. 9(a). In a conventional antiferromagnet, the low-field susceptibility parallel to the staggered moment is zero.[18] However, in La_2CuO_4 the presence of the antisymmetric exchange causes χ_c, the susceptibility for $\mathbf{H}\|\mathbf{c}$, to be nonzero:

$$\chi_c=\chi_0H_1/(H_1+H_2)\ .$$

The magnetization has a jump at $H=H_1$; this jump is

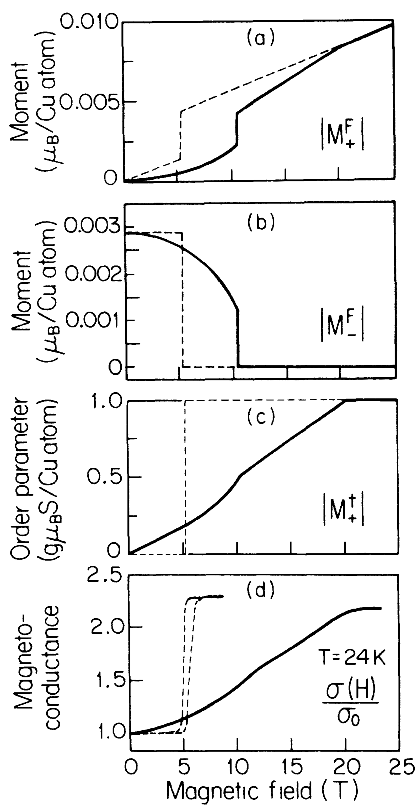

FIG. 9. Calculated order parameters and low-temperature magnetoconductance as a function of magnetic field for spin-flop transition (solid curves) and weak ferromagnetic transition (dashed curves). (a) Calculated uniform ferromagnetic moment; (b) calculated difference of the ferromagnetic moments in adjacent layers; (c) calculated interlayer order parameter for $\tau\|\mathbf{c}$; (d) measured magnetoconductance, $T=24$ K. For the theoretical curves the critical fields were chosen to agree with experiment.

broadened appreciably if the field deviates from the **c** axis by only a few degrees. The uniform moment has a knee at H_2, above which it has a linear field dependence $M(H)=\chi_0(H+H_M)$. We emphasize that this is a zero-temperature calculation. The field dependence of the uniform moment (Fig. 3) agrees qualitatively with the calculated $M_+^F(H)$ (corrected for twinning), although, since the measurement was done at $T=77$ K, the features are broadened and the values of the critical fields have shifted according to the phase diagram of Fig. 2.

B. Magnetoresistance

The most intriguing aspect of this work is the high sensitivity of the conductivity to the magnetic order. We demonstrate next that the magnetoconductance is proportional to $M_+^\dagger$, the total staggered moment with propagation vector in the [0 0 1] direction, $\tau\|\mathbf{c}$.

The spin flop is similar to the WF transition in this respect: In both transitions the relative order of interlayer nearest-neighbor spins changes from antiferromagnetic at zero field to ferromagnetic at high field. We have, therefore, calculated various quantities which change at these transitions. The sum $M_+^F=(M_1^F+M_2^F)/2$ and difference $M_-^F=(M_1^F-M_2^F)/2$ of the ferromagnetic moments in two adjacent layers are plotted in Fig. 9(a) and 9(b), respectively. As shown in neutron scattering experiments,[7] the sum and difference of the staggered moments are the three-dimensional order parameters for the cases that τ is in the **c** and **a** directions, respectively. They are simply related by

$$M_+^\dagger=(M_1^\dagger+M_2^\dagger)/2=g\mu_BS\sin\xi$$

and

$$M_-^\dagger=(M_1^\dagger-M_2^\dagger)/2=g\mu_BS\cos\xi\ .$$

$M_-^\dagger$ and $M_+^\dagger$ are the components of the staggered moment per unit cell with propagation vector $\tau\|\mathbf{a}$ and $\tau\|\mathbf{c}$, respectively. Equivalently, $M_-^\dagger$ and $M_+^\dagger$ measure the relative antiferromagnetic and ferromagnetic alignments respectively of the interlayer nearest-neighbor spins. We plot only $M_+^\dagger$ in Fig. 9(c). The experimental data at $T=24$ K are plotted in Fig. 9(d) as magnetoconductance.

The magnetoconductance does not follow the field dependence of the total moment. This is seen clearly in the case $\mathbf{H}\|\mathbf{b}$ [Fig. 9(a)], where $M_+^F(H)$ has a finite slope both above and below the transition, whereas the MR is independent of field in these regions.

For $\mathbf{H}\|\mathbf{b}$, M_-^F is independent of field above and below the transition [Fig. 9(b)]. Its field dependence is consistent with the heuristic idea that the conductivity is enhanced when the canting in adjacent layers becomes identical. However, in the case of the spin-flop transition, the calculated M_-^F indicates that the layers become equivalent at H_1. (For $H>H_1$, the $\mathbf{M}_i^F$ in all layers point in the direction of the applied field). In contrast, the observed magnetoconductance does not saturate at H_1; in fact, the conductivity $\sigma(H)$ becomes independent of field only for $H>H_2$.

A comparison of Figs. 9(c) and 9(d) shows that the magnetoconductance $\Delta\sigma/\sigma_0$ is proportional to $M_+^\dagger$, for both the spin-flop and the WF transitions. Note that at the highest fields, $\mathbf{M}_i^\dagger \| \mathbf{c}$ for the WF transition, whereas $\mathbf{M}_i^\dagger \| \mathbf{b}$ for the spin-flop transition. The fact that the magnitude of the magnetoconductance is the same in both situations (see Fig. 4) indicates that the holes are not sensitive to the direction of the staggered moment, but only to the relative interlayer *ordering* of the Cu spins.

We discuss next the anisotropic conductivity of La_2CuO_4, which is large at high temperature.[10] At low temperature, σ_a/σ_b, the ratio of the dc conductivities in the in-plane to that in the out-of-plane direction, is weakly dependent on temperature. Above $T \approx 50$ K the anisotropy increases strongly. These results, together with measurements of the Hall effect,[10] indicate that at high temperature the conductivity is dominated by thermal activation of carriers into a band of highly anisotropic states. At low temperature the dominant transport mechanism is thermally assisted tunneling between localized states.[10,11] Since hopping in an anisotropic medium is essentially three dimensional,[20] the total conductivities can be written:

$$\sigma_b = \sigma_{bA} + \sigma_h , \quad \sigma_a = \sigma_{aA} + \gamma\sigma_h , \tag{6}$$

where σ_{bA} and σ_{aA} are the activated components of σ_b and σ_a, respectively, σ_h is the hopping component, and $\gamma = (\xi_a/\xi_b)^2$, where ξ_a and ξ_b are the localization lengths in the in-plane and out-of-plane directions, respectively.[20]

If only the hopping component contributes to the MR, one expects, $\Delta\sigma_b/\Delta\sigma_a = 1/\gamma$ independent of temperature, whereas one expects the anisotropy in the *relative* MR,

$$(\Delta\sigma_b/\sigma_b)/(\Delta\sigma_b/\sigma_a) = (1/\gamma)(\sigma_a/\sigma_b) ,$$

to be strongly T dependent at high T. If, alternatively, the MR arises from a change in the mobility of the states at the band edge, writing $\sigma_a = ne\mu_a$ and $\sigma_b = ne\mu_b$, one expects both

$$\Delta\sigma_b/\Delta\sigma_a = \Delta\mu_b/\Delta\mu_a$$

and

$$(\Delta\sigma_b/\sigma_b)/(\Delta\sigma_a/\sigma_a) = (\mu_a\Delta\mu_b)/(\mu_b\Delta\mu_a)$$

to be weakly T dependent.

We observe (Fig. 5) that $\Delta\sigma_a/\Delta\sigma_b$ is roughly T independent, whereas

$$(\Delta\sigma_b/\sigma_b)/(\Delta\sigma_a/\sigma_a)$$

is not. Furthermore, the values of γ derived from the low-T value of $\sigma_a/\sigma_b(\sim 15)$ and from $\Delta\sigma_a/\Delta\sigma_b(\sim 13)$ agree very well. Thus Eq. (6) provides a good description of the conductivity tensor and the magnetic order appears to influence primarily the hopping conductivity. Measurements of the ac conductivity and the frequency-dependent dielectric constant at the WF transition confirm this conclusion.[11] Since the in-plane band conductivity σ_{aA} is almost purely 2D, it is not surprising that it is insensitive to the interlayer magnetic ordering. However, it is surprising that this also appears to be the case for σ_{bA}.

The low-T magnetoconductance, which is dominated by hopping, is proportional to $M_+^\dagger$ at fixed T. The overall change in $M_+^\dagger$ with field at any T is just $M_-^\dagger(0)$, the order parameter at zero field, at that T. One would therefore expect $\Delta\sigma_h/\sigma_h$, the overall change in the hopping conductivity, to scale with the zero-field interlayer order parameter, $M_-^\dagger$, when T is varied. The overall change of σ_b, plotted in Fig. 4, is

$$\Delta\sigma_b/\sigma_b = \Delta\sigma_h/(\sigma_{bA} + \sigma_h) .$$

This quantity is roughly equal to $\Delta\sigma_h/\sigma_{bA}$ at high T. We find that at high temperature $(\Delta\sigma_b/\sigma_b)|M_-^\dagger|^{-1}$ is indeed proportional to $1/\sigma_{bA}$. This explains why $\Delta\sigma_b/\sigma_b$ decreases much faster than $|M_-^\dagger|$ with increasing temperature.[6]

V. CONCLUSIONS

Using magnetoresistance, we have mapped out the phase diagram for the spin-flop transition in insulating La_2CuO_{4+y}. The peculiar nature of the antisymmetric exchange makes the spin-flop transition complicated; however, the measurements do provide values of both the out-of-plane anisotropy in the nearest-neighbor exchange, and the antisymmetric exchange. We have confirmed previous results showing that the in-layer nearest-neighbor is described, to a high degree of accuracy, by the Heisenberg Hamiltonian. The most important conclusion of this work is that the large magnetoconductance arises from the interlayer hopping component of the conductivity, and that it is proportional to $M_+^\dagger$, the staggered moment with $\tau \| \mathbf{c}$.

Despite this thorough characterization of the magnetoconductance, its microscopic mechanism is still a mystery. The large MR is seen only in the hopping conductivity which varies as $\exp[-R/(\xi_a^2\xi_b)^{1/3}]$ where R is the hopping distance and ξ_a and ξ_b are the localization lengths. The effect on the conductivity of a change of R or ξ_a, ξ_b with field will therefore be amplified by a factor $R/(\xi_a^2\xi_b)^{1/3}$. However, estimates based on the theory of Shklovskii for hopping in an anisotropic medium[20] indicate that, even with this amplification factor,[21] $R/(\xi_a^2\xi_b)^{1/3}$ must change by $\gtrsim 20\%$ to account for the observed change in conductivity. We emphasize that the change in the magnetic order from $\tau \| \mathbf{a}$ to $\tau \| \mathbf{c}$ is a very subtle one, since the orthorhombic distortion is only $(|\mathbf{c}|-|\mathbf{a}|)/|\mathbf{c}| \approx 0.5\%$.[8] Furthermore, in nearly all models of hopping conductivity,[22] the magnetoconductance is predicted to be sensitive to the *uniform* magnetic moment because of the overlap of the spin parts of the initial and final eigenstates. The observed proportionality between the magnetoconductance and $M_+^\dagger$ is unique and shows that the coupling between the charge and spin degrees of freedom is quite unusual.

ACKNOWLEDGMENTS

This work was supported by National Science Foundation (NSF) Grant Nos. DMR84-15336 and DMR87-19217; experiments were performed at the Francis Bitter

National Magnet Laboratory, which is supported at the Massachusettes Institute of Technology by the National Science Foundation. Research at Brookhaven was supported by the Division of Materials Science, U.S. Department of Energy, under Contract No. DE-AC02-CH00016. We thank S. Foner and E. J. McNiff, Jr. for help in the measurement of the uniform moment. We gratefully acknowledge helpful discussions with J. D. Axe, A. G. Swanson, and B. L. Brandt.

APPENDIX

The measurements and analysis presented in this paper and in Ref. 6 reveal several features in the magnetism and transport in the lightly doped regime which may be relevant to the superconductivity in $La_{2-x}Ba_xCuO_4$ and $La_{2-x}Sr_xCuO_4$. First, the transport measurements at low temperatures reveal an extraordinary sensitivity of the interlayer hopping conductivity to the relative interlayer ordering of the Cu^{2+} spins. Indeed, as we have emphasized in the conclusion section of this paper, we do not properly understand this sensitivity. Second, the experiments show that the largest correction to the $Cu^{2+}-Cu^{2+}$ Heisenberg exchange in La_2CuO_4 is the antisymmetric exchange. In pure or lightly doped La_2CuO_4 the effects of the antisymmetric exchange are quite subtle; specifically, it causes a canting[6] of the Cu^{2+} spins by $\sim 0.17°$. As we shall discuss in the following, in the more heavily doped samples the effects may be much more substantial.

There is a number of features of the superconductivity in the single layer CuO_2 materials such as $La_{2-x}Sr_xCuO_4$ which seem unique, at least as compared to double or triple-layer CuO_2 superconductors like $YBa_2Cu_3O_7$ and $Bi_2Sr_2CaCu_2O_{8-x}$. First, in $La_{1.85}Sr_{0.15}CuO_4$ for example, the superconducting T_c is extraordinarily sensitive to pressure rising from <40 K to nearly 50 K with the application of ~ 20 kbars pressure.[23] The multilayer materials show much less dramatic pressure dependences.[24] It seems likely that this reflects an unusual sensitivity of the T_c's in $La_{1.85}Sr_{0.15}CuO_4$-type materials to the interlayer coupling; concomitantly any modification of the interlayer coupling may affect T_c drastically. Second, Axe *et al.*[25] and others[26] have recently shown that $La_{2-x}Ba_xCuO_4$ with $x \simeq 0.12$ exhibits two polytypes. One has the same orthorhombic structure as $La_{2-x}Sr_xCuO_4$ and has superconducting T_c's of ~ 25 K. The second has a tetragonal structure with four La_2CuO_4 units per primitive cell. There is evidence that in the latter phase T_c may be less than 5 K.[25] In our view this dramatic difference in superconducting transition temperatures in these two phases which have only subtly different crystal structures represents a challenge to any model for the superconductivity.

It is useful, therefore, to consider possible differences in the Hamiltonians in the two structures. The *Cmca* structure of orthorhombic $La_{2-x}(Ba,Sr)_xCuO_4$ has two formula units per primitive cell; this structure is generated by condensation of one of the two degenerate *X*-point soft phonons with wave vectors in *Cmca* notation at (1,0,0) and (0,0,1).[27] This leads to a staggered rotation of the octahedra about an **a** axis. As shown by Thurston *et al.*,[27] the (0,0,1) zone boundary rotary phonon remains quite low in energy: $\sim$4meV in $La_{1.86}Sr_{0.14}CuO_4$. Axe *et al.*[25] argue that the low-temperature tetragonal phase in $La_{1.88}Ba_{0.12}CuO_4$ is generated by condensation of this second phonon leading to the $P4_2/ncm$ structure. To first order, this structure may be thought of as being generated by rotations of the CuO_6 octahedra about the tetragonal (1,0,0) and (0,1,0) axes in successive layers, that is, the CuO_6 rotation axis alternates layer by layer.

Since the *X*-point (0,0,1) phonon branch only changes its energy over a small portion of the Brillouin zone, it is difficult to believe that a lattice dynamical mechanism can account for the drastic reduction in T_c in $La_{1.88}Ba_{0.12}CuO_4$. Similarly, since the net CuO_6 rotation angle in the *Cmca* and $P4_2/ncm$ phases is the same, the electronic structure should not change significantly. On the other hand, since the antisymmetric exchange is generated by the rotation itself, it will differ in a fundamental way in the two phases. It is therefore pertinent to explore the possible role of the antisymmetric exchange in the superconducting samples.

As we noted above, in pure La_2CuO_4 the antisymmetric exchange causes a canting of the Cu^{2+} spins by $\sim 0.17°$. However, recent neutron scattering experiments[28] have revealed that in $La_{2-x}Sr_xCuO_4$ with $x \geq 0.07$, the short-range spin ordering is markedly incommensurate. Indeed, nearest neighbor spins are misoriented by $\sim 30°$ relative to the antiferromagnetic alignment in pure La_2CuO_4. Furthermore, for both static and mobile holes,[29] the Cu^{2+} spins in the neighborhood of the hole are noncollinear with quite large effective canting angles. For both cases the antisymmetric exchange may become quite significant. For order of magnitude purposes we estimate for superconducting concentrations

$$E_{A/S} \sim zJ_{bc}S[\phi(x)/\phi(0)]\tfrac{1}{2}(\xi/a_{\rm NN})^2\sin(30°) \simeq 40\ °{\rm K}\ .$$

Here

$$(\xi/a_{\rm NN}) \simeq 4 \text{ and } [\phi(x)/\phi(0)] \simeq \tfrac{1}{2}\ ,$$

where $\phi(x)$ is the rotation angle of the CuO_6 octahedra as a function of Sr content x. Thus the antisymmetric exchange energy will become significant for a two-dimensional correlated region of Cu^{2+} spins for temperatures of order 40 K. This means that in a correlated area the spins will be preferentially oriented in the plane perpendicular to the CuO_6 rotation axis. In the *Cmca* structure the rotation direction is identical in successive CuO_2 layers. However, in the tetragonal $P4_2/ncm$ structure the CuO_6 rotation axis alternates by 90° between successive layers. This in turn implies that the Cu^{2+} spins including most especially those surrounding the holes will be oriented at $\sim 90°$ relative to each other in successive CuO_2 sheets. The magnetoconductance results reported in this paper imply that this will in turn reduce the coupling between the sheets and hence should act to reduce T_c.

Clearly, therefore, the antisymmetric exchange could play an important role in the $La_{2-x}Ba_xCuO_4$ system. Certainly the pressure dependence of T_c suggests that the coupling between the sheets is quite important. Furthermore, dT_c/dP is large only in the orthorhombic phase; indeed in purely tetragonal ($I4/mmm$) $La_{1.85}Sr_{0.15}CuO_4$ above 20 kbar T_c is nearly independent of pressure.[23,30] It is, however, quite surprising that T_c appears to be so low in the $P4_2/ncm$ phase. Indeed in a Kosterlitz-Thouless picture one would expect that as the coupling between the CuO_2 planes went to zero T_c would saturate at the two-dimensional Kosterlitz-Thouless value. If the speculations presented here are correct then this would imply that the intrinsic superconductivity is a three-dimensional effect or, at the minimum, requires at least two correlated CuO_2 sheets.

Neutron scattering experiments on single-domain samples could test the ideas discussed here concerning the spin correlations. Transport measurements on single crystal $La_{1.88}Ba_{0.12}CuO_4$ through the low-temperature orthorhombic-tetragonal transition would reveal any anomalous decrease in the interlayer conductivity. Such measurements as a function of pressure would also be quite informative.

---

*Also at Department of Physics, Massachusetts Institute of Technology, Cambridge, MA 02139.

†Present address: AT&T Bell Laboratories, Murray Hill, NJ.

[1]J. G. Bednorz and K. A. Müller, Z. Phys. B **64**, 189 (1986).

[2]G. Shirane *et al.*, Phys. Rev. Lett. **59**, 1613 (1987); Y. Endoh *et al.*, Phys. Rev. B **37**, 7443 (1988).

[3]S. Chakravarty, B. I. Halperin, and D. R. Nelson, Phys. Rev. Lett. **60**, 1057 (1988).

[4]C. J. Peters *et al.*, Phys. Rev. B **37**, 9761 (1988).

[5]R. T. Collins *et al.*, Phys. Rev. B **37**, 5817 (1988).

[6]Tineke Thio *et al.*, Phys. Rev. B **38**, 905 (1988).

[7]M. A. Kastner *et al.*, Phys. Rev. B **38**, 6636 (1988).

[8]R. J. Birgeneau *et al.*, Phys. Rev. Lett. **59**, 1329 (1987).

[9]P. J. Picone, H. P. Jenssen, and D. R. Gabbe, J. Cryst. Growth **85**, 576 (1987); **91**, 463 (1988).

[10]N. W. Preyer *et al.*, Phys. Rev. B **39**, 11 563 (1989).

[11]C. Y. Chen *et al.*, Phys. Rev. Lett. **63**, 2307 (1989).

[12]Schirber *et al.*, Physica **152C**, 121 (1988); J. W. Rogers, Jr. *et al.*, Phys. Rev. B **38**, 5021 (1988).

[13]H. C. Montgomery, J. Appl. Phys. **42**, 2971 (1971).

[14]R. R. P. Singh *et al.*, Phys. Rev. Lett. **62**, 2736 (1989).

[15]I. Dzyaloshinsky, J. Phys. Chem. Solids **4**, 241 (1958).

[16]T. Moriya, Phys. Rev. **120**, 91 (1960).

[17]A. S. Borovik-Romanov *et al.*, Pis'ma Zh. Eksp. Teor. Fiz. **47**, 600 (1988) [JETP Lett. **47**, 697 (1988)].

[18]T. Nagamiya, K. Yosida, and R. Kubo, Adv. Phys. **4**, 1 (1955); J. M. Kosterlitz, D. R. Nelson, and M. E. Fisher, Phys. Rev. B **13**, 412 (1976).

[19]W. P. Wolf, J. Phys. (Paris) Colloq. **32**, C1-26 (1971).

[20]B. I. Shklovskii, Fiz. Tekh. Poluprovodn. **11**, 2135 (1977) [Sov. Phys.—Semicond. **11**, 1253 (1977)].

[21]M. A. Kastner *et al.*, Phys. Rev. B **37**, 111 (1988).

[22]N. F. Mott and E. A. Davis, *Electronic Processes in Non-Crystalline Materials,* 2nd ed. (Oxford University Press, Oxford, 1979).

[23]C. W. Chu *et al.*, Science **235**, 567 (1987); D. Erskine *et al.*, J. Mater. Res. **2**, 783 (1987); S. Yomo *et al.*, J. Appl. Phys. **26**, L603 (1987).

[24]P. H. Hor *et al.*, Phys. Rev. Lett. **58**, 911 (1987); K. Murata *et al.*, Jpn. J. Appl. Phys. **26**, L471 (1987); A. Driessen *et al.*, Phys. Rev. B **36**, 5602 (1987); R. J. Wijngaarden *et al.*, Physica **152C**, 140 (1988).

[25]J. D. Axe *et al.*, Phys. Rev. Lett. **62**, 2751 (1989).

[26]M. Sera *et al.*, Solid State Commun. **69**, 851 (1989); N. Yamada *et al.*, *ibid.* **70**, 1151 (1989).

[27]T. R. Thurston *et al.*, Phys. Rev. B **39**, 4327 (1989), and references therein.

[28]R. J. Birgeneau *et al.*, Phys. Rev. B **39**, 2868 (1989).

[29]D. M. Frankel, R. G. Gooding, B. I. Shraiman, and E. D. Siggia (unpublished).

[30]H. J. Kim and R. Moret, Physica **156C**, 363 (1988).